

Stability analysis of three-dimensional trusses

M. Greco and W.S. Venturini*

University of São Paulo, São Carlos School of Engineering, Department of Civil Engineering, São Carlos, SP, Brazil

Abstract

This paper presents a new geometric nonlinear formulation for stability analysis involving 3D trusses. The proposed formulation is based on the Finite Element Method (FEM) and uses nodal positions rather than nodal displacements to describe the problem. The strains are computed directly from the proposed position concept, using a Cartesian co-ordinate system fixed in space. The proposed formulation is simple and the validation of the model is shown in the example section. Four examples are presented here to validate the formulation.

Keywords: nonlinear analysis, stability, FEM, space trusses

1 Introduction

Structural stability is an important topic in nonlinear analysis. The current tendency of using more slender structures with higher strength makes the stability analysis a subject of fundamental importance. Stability loss can be distinguished by bifurcations in nonlinear differential equations that govern engineering problems. Critical points may arise, especially in problems with severe geometrical nonlinearities, as in the case of slender structures. The study of structural stability is based on the critical points identification. The critical points are defined as limit points or bifurcation points. In these two cases, both the gradient of the strain energy and the Laplacian of the strain energy are singular. In the bifurcation point at least one eigenvalue of the Hessian matrix is null.

There are indirect and direct numerical methods for stability analysis. Regarding the indirect methods, critical points are found using approximate techniques based on particular parameters, for example the matrix determinant. In the imminence of the bifurcation, a position (or force) perturbation is introduced, searching for possible secondary solution paths. This scheme is called the path-following technique. Formulations for indirect methods (adopted in this paper) can be found in Shi and Crisfield [20], Wagner and Wriggers [21] and Kleiber and Wozniak [12]. Concerning the direct methods, the conditions of existence of the critical points are directly introduced into the formulation by creating an extended system of equations. The bifurcation point is straightforward found, as well as the eigenvector associated with the singular condition.

*Corresp. author email: venturin@sc.usp.br

Nomenclature

U	Strain energy
Π	Total potential energy
P	Potential energy
σ	Stress tensor
ε	Nonlinear engineering strain
U	Specific strain energy
E	Young's modulus
V	Volume of the body
A	Cross-section area
X	Set of positions independent of each other
L	Element length
ds	Element fiber
F	Applied forces
ξ	Dimensionless co-ordinate
$f_i(X_j)$	Gradient of the strain energy
$g(X)$	Residual vector
N	Normal force of the bar
ω_1	First eigenvalue
ϕ	Eigenvector
$[H]$	Hessian matrix

The strain energy gradient is changed at the bifurcation point depending on the required path response. Formulations for direct methods can be found in Battini et al. [2], Oñate and Matias [17], Shi and Crisfield [20], Wriggers and Simo [22] and Wriggers et al. [23].

The main objective of this paper is to present a new and simple geometric nonlinear formulation based on the Finite Element Method appropriate for space truss stability analysis. The structural element known as space truss is widely used in Structural Engineering, particularly in designs involving large spans. Numerical modeling of space structures involves nonlinearity due to geometrical changes and nonlinearity introduced by the behavior and instability of materials. Several formulations to solve geometric nonlinear problems in structures using finite elements can be found in the specialized literature, as the formulations given in Bathe [1] and Crisfield [6]. These formulations differ in their coordinate descriptions as can be seen in Gadala et al. [8]. The Lagrangian description, which measures the configurative changes in structures from a point of reference in space, can be total or updated. If the reference is updated during the element deformation the formulation is called updated, as shown in Meek and Tan [14]. If the reference is the initial configuration established during the element deformation, then the formulation is called total, as shown in Mondkar and Powell [15]. The corotational formulation, commonly employed to carry out geometrical nonlinear analysis, uses local coordinate systems to consider

curvature effects in finite elements. The corotational formulation can be found in Crisfield [5]. Other interesting procedures to solve geometric nonlinear problems are related with the vector iteration methods, such as the dynamic relaxation and the first order conjugate gradient found in Papadrakakis [18]. Hessian matrix computing is not required in the vector iteration methods; the convergence is obtained by operating with vectors.

The present study uses a simple engineering description to present a geometrical nonlinear formulation for space trusses based on position description as previously shown in Coda and Greco [4].

2 Formulation for large nonlinear displacements

For a conservative structural problem associated with a reference system fixed in space, the strain energy (U) of the structure can be written after the onset of the structural deformation. The total potential energy (Π) is written in terms of the strain energy and the applied forces (P) potential energy. The principle of minimum potential energy will be used. Thus, let us write the total potential energy (Π) as follows,

$$\Pi = U - P \quad (1)$$

The strain energy can be written for the initial volume V as:

$$U = \int_V u dV = \int_V \int_{\varepsilon} \sigma d\varepsilon dV = \int_V \int_{\varepsilon} E \varepsilon d\varepsilon dV = \int_V \frac{1}{2} E \varepsilon^2 dV \quad (2)$$

In Eq. (2), the term σ is defined as the engineering stress, i.e., the conjugated stress related with the proposed nonlinear engineering strain (ε). The strain energy is assumed to be zero at an initial position, defined as the non-deformed position. The variable u is the specific strain energy, while the potential energy of the applied forces is given by:

$$P = \sum FX \quad (3)$$

where X is the set of positions independent of each other, which may be occupied by a body material point. It is interesting to note that the applied force potential energy may not be zero in the initial configuration. Thus, the total potential energy is written as:

$$\Pi = \frac{E}{2} \int_V \varepsilon^2 dV - \sum FX \quad (4)$$

In order to carry out the integral indicated in Eq. (4), the geometry of the studied body should be mapped to know its relation with the adopted strain measurement. Figure 1 gives the general kinematics for a space truss element.

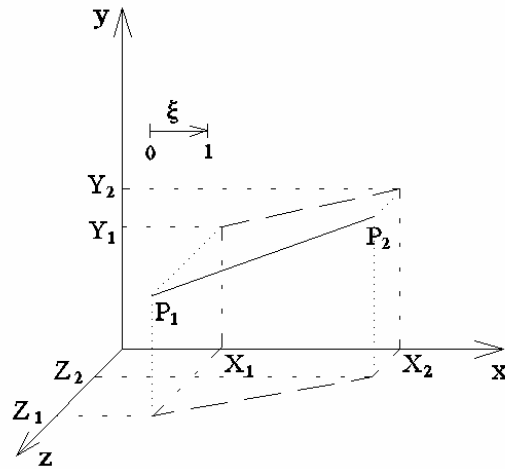


Figure 1: Space truss element

The truss bar kinematics shown in Figure 1 can be parameterized in terms of a dimensionless co-ordinate ξ (varying from 0 to 1).

$$x = X_1 + (X_2 - X_1)\xi \quad (5)$$

$$y = Y_1 + (Y_2 - Y_1)\xi \quad (6)$$

$$z = Z_1 + (Z_2 - Z_1)\xi \quad (7)$$

The longitudinal strain component is the only one considered for this analysis. The initial length is defined by ds_0 that, after the onset of the structural deformation, becomes ds . Thus, the strain measure is given by a Lagrangian variable, the traditional linear deformation, as follows [16]:

$$\varepsilon = \frac{ds - ds_0}{ds_0} \quad (8)$$

At this point it is clear that the proposed formulation is different from the usual geometric nonlinear formulations. The strain measure given by Eq. (8) is the simplest measure found in the literature and adopted here to obtain a geometric nonlinear formulation.

One can transform Eq. (8) into a more appropriate expression dividing the initial and final lengths by $d\xi$ to give:

$$\varepsilon = \frac{ds/d\xi - ds_0/d\xi}{ds_0/d\xi} \quad (9)$$

The values $ds_0/d\xi$ and $ds/d\xi$ can be considered auxiliary stretches computed in terms of the dimensionless co-ordinate ξ .

As usual the initial values $ds_0/d\xi$ can be easily written in terms of partial derivatives as follows:

$$\frac{ds_0}{d\xi} = \left(\sqrt{\left(\frac{dx}{d\xi}\right)^2 + \left(\frac{dy}{d\xi}\right)^2 + \left(\frac{dz}{d\xi}\right)^2} \right)_0 = \left(\sqrt{(X_2 - X_1)^2 + (Y_2 - Y_1)^2 + (Z_2 - Z_1)^2} \right)_0 = l_0 \quad (10)$$

where l_0 is the finite element initial length.

The value $ds/d\xi$ for any instant is given by:

$$\frac{ds}{d\xi} = \sqrt{\left(\frac{dx}{d\xi}\right)^2 + \left(\frac{dy}{d\xi}\right)^2 + \left(\frac{dz}{d\xi}\right)^2} = \sqrt{(X_2 - X_1)^2 + (Y_2 - Y_1)^2 + (Z_2 - Z_1)^2} = l \quad (11)$$

For the proposed formulation the strain energy is obtained by integrating Eq. (2) over the element volume. Then, after carrying out this integral along the element length for a constant cross-section area and taking into account Eqs. (9), (10) and (11), one has:

$$U = l_0 \int_0^1 \frac{EA}{2} \varepsilon^2 d\xi = \int_0^1 l_0 u_t d\xi \quad (12)$$

The integral in equation (12) along the bar length (along ξ) yields the exact solution. The variable u_t , representing the integral of the specific strain energy (u) over the cross-section area, was adopted to make the computations easier.

Since the strain energy is written in terms of nodal positions, the Total Potential Energy can be differentiated to obtain the equilibrium equation. Thus, Eq. (4) is reorganized as follows:

$$\Pi = l_0 \int_0^1 u_t d\xi - F_{X_1} X_1 - F_{Y_1} Y_1 - F_{Z_1} Z_1 - F_{X_2} X_2 - F_{Y_2} Y_2 - F_{Z_2} Z_2 \quad (13)$$

where $(X_1, Y_1, Z_1, X_2, Y_2, Z_2)$ are nodal positions and $(F_{X_1}, F_{Y_1}, F_{Z_1}, F_{X_2}, F_{Y_2}, F_{Z_2})$ are their conjugate forces. Since there is no singularity in the strain energy integral, one can differentiate Eq. (13) in terms of nodal positions with three degrees of freedom per node ($i = 1 - 6$), as follows:

$$\frac{\partial \Pi}{\partial X_i} = l_0 \int_0^1 \frac{\partial u_t}{\partial X_i} d\xi - F_i = 0 \quad (14)$$

To simplify the calculations, the following rule between classical co-ordinates representation and index notations is used: $(X_1, Y_1, Z_1, X_2, Y_2, Z_2) = (1, 2, 3, 4, 5, 6)$.

The numerical strategy is to carry out the derivatives inside the integrals and then carry out the integrals analytically. As can be seen, the resulting integrated values are nonlinear in terms of nodal positions. The above system of equations is then written using indicial notation (free index $i = 1 - 6$ and dummy index $j = 1 - 6$):

$$\frac{\partial \Pi}{\partial X_i} = g_i(X_j, F_i) = f_i(X_j) - F_i = 0 \quad (15)$$

or using vector representation,

$$g(X) = f - F = 0 \quad (16)$$

For conservative forces, whose work does not depend on the path, the gradient of the total strain energy ($f_i(X_j)$) depends only on the nodal variable positions.

It is important to note that, in this study, the applied forces are independent of space. The vector function $g(X)$ is nonlinear in terms of nodal positions. To solve Eq. (16), one can use the Newton-Raphson procedure,

$$g(X) \cong 0 = g(X_0) + \nabla g(X_0) \Delta X \quad (17)$$

where X and X_0 are vectors representing current and initial positions, respectively.

The Hessian matrix $\nabla g(X_0)$ can be evaluated from Eqs. (13) and (15), as follows:

$$\nabla g(X_0) = g_{i,k}(X_0) = f_{i,k}(X_k) - F_{i,k} \quad (18)$$

where $i = 1 - 6$ and $k = 1 - 6$ represent parametric positions. Thus, the following expression can be found:

$$\nabla g(X_0) = l_0 \int_0^1 u_{t,ik} d\xi \Big|_{X_0} \quad (19)$$

To solve Eq. (17) requires computing $g(X_0)$,

$$g(X_0) = l_0 \int_0^1 u_{t,i} d\xi \Big|_{X_0} - F_i \quad (20)$$

The iterative Newton-Raphson process is summarized as follows:

1. Assume X_0 as the initial configuration (non-deformed). Compute $g(X_0)$ following Eq. (20).
2. For this X_0 , find the Hessian matrix and the gradient of g at X_0 using Eq. (19).
3. Solve the system of Eqs. (17) to find ΔX .
4. Update position $X_0 = X_0 + \Delta X$. Return to step 1 until ΔX is sufficiently small.

Theoretically, the process is not incremental. However, dividing the total loading (or prescribed position) into cumulative steps helps us to start the iterative procedure at a position closer to the final expected result and therefore reducing the number of iterations.

3 Practical procedure

In order to implement the described formulation, the derivatives of u_t ($u_{t,i}$ and $u_{t,ik}$) are computed according to Eq. (12) rewritten as follows:

$$l_0 u_t = \frac{EA l_0}{2} \left(\frac{\sqrt{B}}{l_0} - 1 \right)^2 \quad (21)$$

where:

$$B = (X_2 - X_1)^2 + (Y_2 - Y_1)^2 + (Z_2 - Z_1)^2 \quad (22)$$

The first derivative from Eq. (21) is given by:

$$l_0 u_{t,i} = \frac{EA}{2l_0} \left(1 - \frac{l_0}{\sqrt{B}} \right) B_{,i} \quad (23)$$

Differentiating Eq. (23) the second derivative of u_t is obtained:

$$l_0 u_{t,ik} = \frac{EA}{2l_0} \left[\frac{l_0 B_{,i} B_{,k}}{2 (\sqrt{B})^3} + \left(1 - \frac{l_0}{\sqrt{B}} \right) B_{,ik} \right] \quad (24)$$

The derivatives of B ($B_{,i}, B_{,k}$ and $B_{,ik}$) in Eqs. (23) and (24) are evaluated from Eq. (22).

With these results, all necessary nodal variables ($X_1, Y_1, Z_1, X_2, Y_2, Z_2$) can be evaluated using the Newton-Raphson procedure for a given position, i.e.,

1. Computing value B and their derivatives: $B_{,i}$, $B_{,k}$ and $B_{,ik}$.
2. Computing $u_{t,i}$ and $u_{t,ik}$ for each finite element.
3. Cumulate all values, find the first derivative of the energy and its gradient (Hessian matrix) and then solve the problem as above.

It should be noted that no co-ordinate transformation has been performed so far, because no transformation is required between the local and global system of co-ordinates. All the derivatives are found in a one-dimension co-ordinate system.

The normal forces along the elements are evaluated by integrating the stress filed over the cross-section, i.e.:

$$N = \int_A \sigma dA = \int_A E \left(\frac{\sqrt{B}}{l_0} - 1 \right) dA = \int_A E \left(\frac{l}{l_0} - 1 \right) dA \quad (25)$$

4 Equilibrium bifurcation

The equilibrium bifurcation problem is characterized by a qualitative change of the equilibrium type when a certain critical condition is reached. The proposed formulation considers possible critical points in the response, where the strain energy becomes singular ($DET [H] = 0$) with at least one eigenvalue null ($\omega_1 = 0$). In a bifurcation point both the strain energy and the smaller eigenvalue associated with the matrix $[H]$ change their signs, i.e.:

$$DET (\nabla g (X_0)) = 0 \quad (26)$$

There are three types of energy states associated with the equilibrium:

- a) Maximum energy: $\frac{\partial^2 \Pi}{\partial X^2} < 0$ (unstable equilibrium state)
- b) Minimum energy: $\frac{\partial^2 \Pi}{\partial X^2} > 0$ (stable equilibrium state)
- c) Constant energy: $\frac{\partial^2 \Pi}{\partial X^2} = 0$ (indifferent equilibrium state)

According to Shi [19] more than one bifurcation point may exist and at a bifurcation point more than two response branches may exist (multiple nullity). At the multiple bifurcation points there are more than one null eigenvalues, while at the simple bifurcation there is only one null eigenvalue (simple nullity). The proposed bifurcation identification criterion is valid only in the case of simple nullity.

Once the instability point is identified, the response branches are founded by a modal perturbation technique, i.e. eigenmode injection [12, 20, 21]. The technique consists of introducing a small perturbation, based on the eigenvector (ϕ) associated with the smallest eigenvalue associated to the initial structural position. Thus, the following expression is applied:

$$X = X_0 + \kappa \phi \quad (27)$$

where κ is an adopted constant used to introduce the perturbation compatible with the dimensions of the structure once the eigenvector is normalized.

The main advantage of the indirect method in comparison with the direct method is its simplicity. In practical structural analysis knowing the exact value of the stability points is not required.

On the other hand, the direct method can be used to compute the exact value of stability points. The direct method is based on three basic equations:

$$l_0 \int_0^1 \frac{\partial u_t}{\partial X} d\xi - \lambda F = 0 \quad (28)$$

$$\nabla g(X_0) \phi = 0 \quad (29)$$

$$\|\phi\| - 1 = 0 \quad (30)$$

where λ is a force factor.

A nonlinear system of equations, based on Eqs. (28) to (30), may be solved using a Newton-Raphson algorithm, as described in Wriggers et al. [23] leading to a non-symmetric and extended system of equations shown in Eq. (31). Wriggers and Simo [22] present some discussions about the direct methods using an alternative symmetric matrix method.

$$\begin{bmatrix} \nabla g(X_0) & -F & 0 \\ \frac{\partial}{\partial X} [\nabla g(X_0) \phi] & \frac{\partial}{\partial \lambda} [\nabla g(X_0) \phi] & \nabla g(X_0) \\ 0 & 0 & \frac{\phi^T}{\|\phi\|} \end{bmatrix} \begin{Bmatrix} \Delta X \\ \Delta \lambda \\ \Delta \phi \end{Bmatrix} = - \begin{Bmatrix} l_0 \int_0^1 \frac{\partial u_t}{\partial X} d\xi - \lambda F \\ \nabla g(X_0) \phi \\ \|\phi\| - 1 \end{Bmatrix} = 0 \quad (31)$$

In the extended systems obtained by using direct methods the Hessian matrix becomes progressively ill-conditioned as the solution approaches the stability point [22]. As an alternative to solve this problem, Wriggers and Simo [22] have used a penalty method to improve the convergence of the modified Newton-Raphson algorithm.

Shi [19] has shown that the direct methods require a good starting vector to achieve convergence. Moreover, converge the critical point is rarely obtained when the starting is made from anywhere in the load displacement space. The direct method demands a good initial prevision (predictor) to reach the convergence. For practical problems, the application of the direct methods is limited because the high accuracy may not be needed or achievable [19].

5 Numerical examples

Four numerical examples are discussed here. The first example is presented with the purpose of validating the proposed formulation, for which an analytical solution is available. The second example involves stability analysis of a plane truss, while the last two examples involve stability analysis of space trusses. The tolerance of 10^{-8} was adopted for all examples. The force factor λ will be adopted to simulate the loading process.

5.1 Three-bar space truss

This simple example shows the severe geometric nonlinear behavior of a space truss. The problem data is presented in Figure 2. In the initial position, the following values were considered: $H = 20cm$ and $L = 500cm$. To run this example, 3 finite elements were used, with a prescribed position increment of $1cm$ applied to the centre node. The following material and geometric parameters were assumed for each member: $E = 20500kN/cm^2$ and $A = 6.53cm^2$.

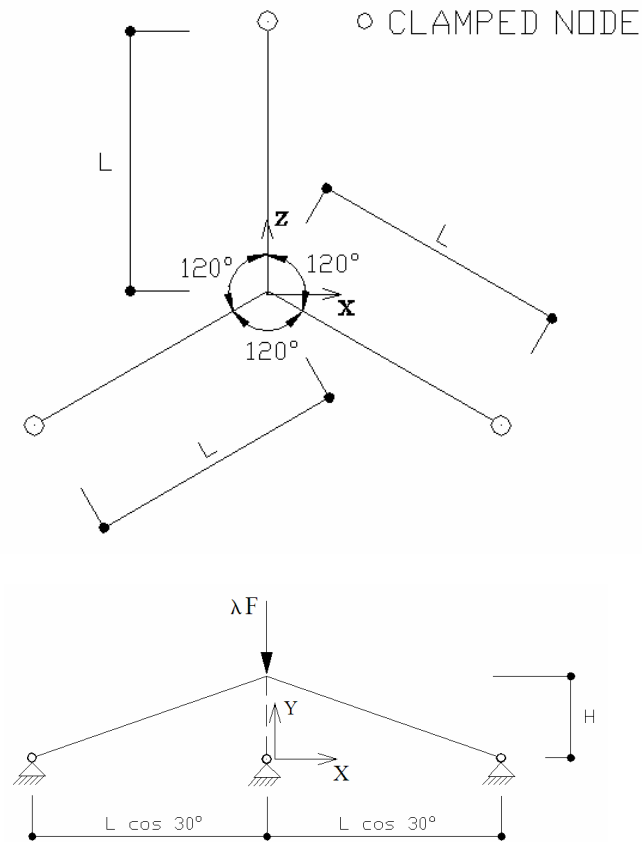


Figure 2: Three-bar space truss front view and top view input data

The analytical solution for this problem is obtained by imposing the equilibrium at the deformed position assuming elastic behavior. For a given position, the equilibrium is obtained considering normal forces in direction Y . The same normal force will appear along the three bars.

The numerical results shown in Figures 3 and 4 are compared with analytical solutions for the vertical position central node and normal forces in the bars. The numerical results for this problem are exactly the analytical solution.

5.2 Stability of a ten-bar plane truss

This example shows the geometric nonlinear behavior of a simple plane truss. The geometry and loading are presented in Figure 5 with co-ordinates given in m . To run this example, 10 finite elements (7 nodes) are used and displacement steps of $0.01cm$ are applied to the central node. The longitudinal stiffness modulus $EA = 5000kN$ is adopted for each member. This example is

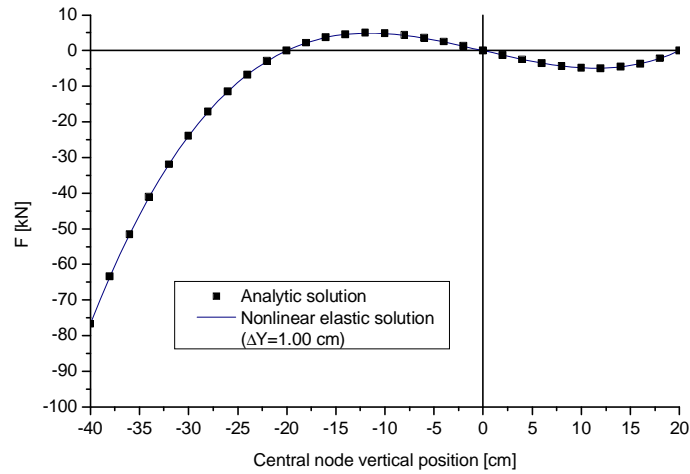


Figure 3: Central node vertical position x force

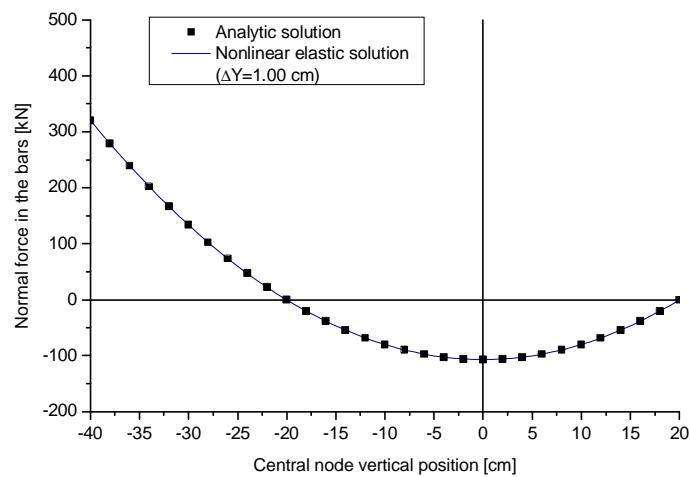


Figure 4: Central node vertical position x normal force in the bars

available in Wriggers et al. [23]. Figure 6 illustrates the numerical responses obtained from the proposed formulation for the geometric nonlinear analysis.

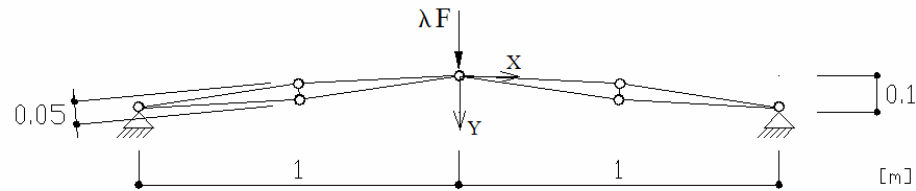


Figure 5: Two-bar plane truss input data

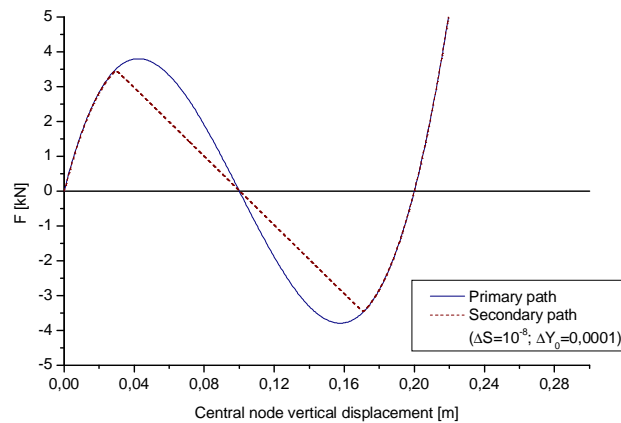


Figure 6: Central node vertical displacement x force

In Figure 6, a bifurcation point is found in the vicinity of the load 3.44 kN , before the first limit point ($F_{LIM} = 3.80\text{ kN}$). The first stability mode (primary solution) is associated with the first limit point, while the second stability mode (secondary solution) is associated with a buckling that occurs at a side of the symmetric structure. The buckling occurs before the limit point which is assumed as the limit load for practical applications.

The primary and the secondary solutions have three points in common, one of them at the central node that has a zero vertical co-ordinate at the equilibrium (as shown in Figure 6). A snapthrough of the central node is observed after the limit point and after the bifurcation point. The obtained results using the proposed formulation are very close to the solutions given by Wriggers et al. [23].

5.3 Stability of a star dome truss

This example shows the geometric nonlinear behavior of a space truss. The geometry and loading are presented in Figure 7 with co-ordinates given in *cm*. Twenty four finite elements with 13 nodes were used to run this example. The displacement at the centre point in the crown top has been applied in steps of 0.05cm . For each bar, constants $E = 10796\text{kN/cm}^2$ and $A = 1.0\text{cm}^2$ were adopted. This example is very common in the nonlinear analysis of space truss specialized literature, e.g., Blandford [3], Krishnamoorthy et al. [13] and Hill et al. [11].

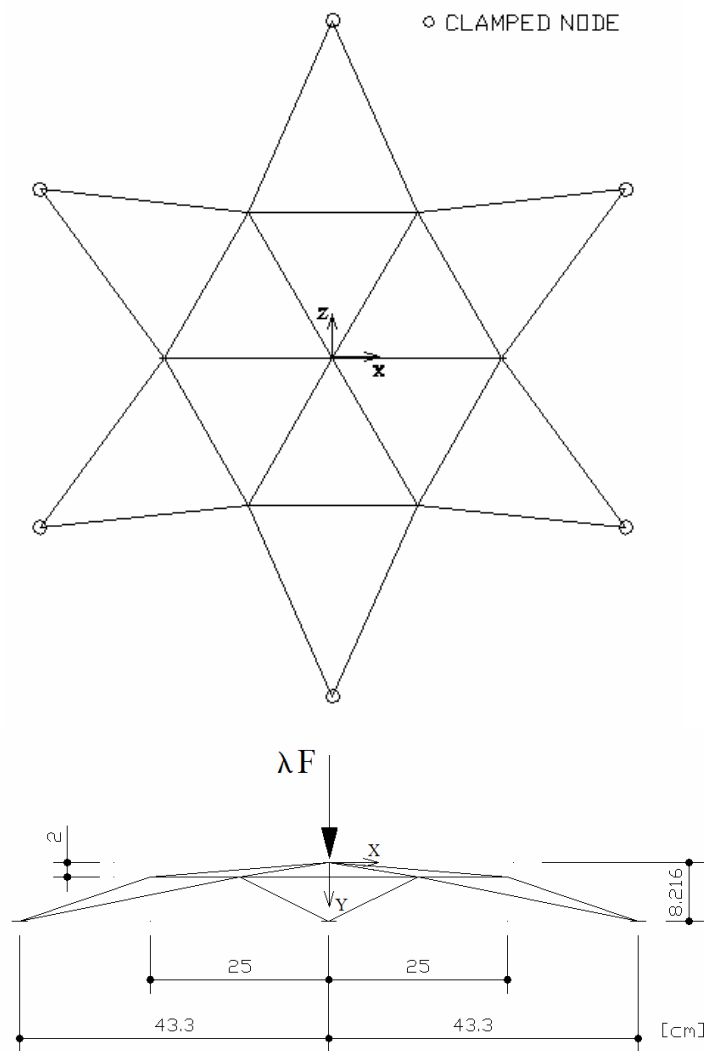


Figure 7: Star dome front and top views input data

The geometric nonlinear solution obtained by using the proposed formulation is given in Figure 8. Two bifurcation points are found. They are near the displacement values of 3.5cm and 13.0cm as shown in Figure 8.

A local truss crown snapthrough is observed after the first limit point, near to the displacement of 0.75cm . The first bifurcation point occurs after the second limit point of the primary solution. Here, only the first buckling mode was considered. The second bifurcation point occurs after the third limit point of the primary solution.

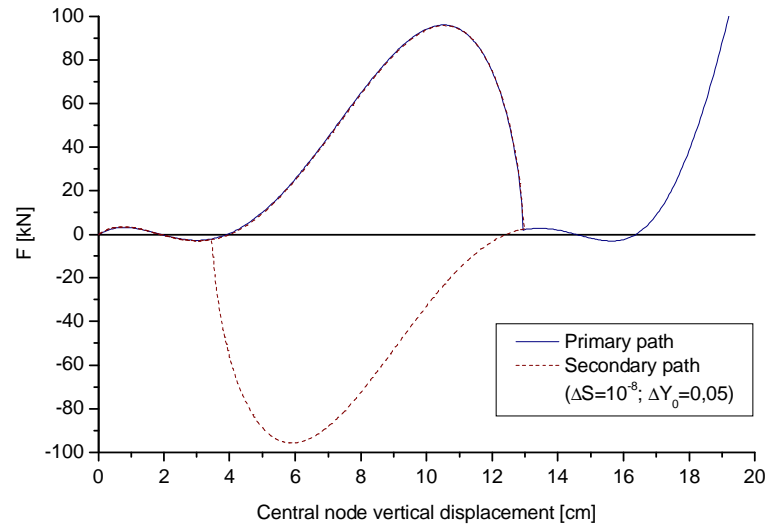


Figure 8: Central node vertical displacement x force

5.4 Stability of a 3D tower

The geometry (values are given in m) of the tower under analysis is presented in Figure 9 where different views were shown. To run this example, 60 finite elements (22 nodes) were used, while the displacement has been applied in the tower top central node using steps of 0.1cm . For three connecting bars at the top, the longitudinal stiffness modulus $EA = 2000\text{kN}$ was adopted, while for the other structural bars $EA = 1000\text{kN}$ was assumed.

In Figures 10 and 11 the displacements of the top node are shown and the captured bifurcation point is in the vicinity of the 26kN load. The bifurcation point, associated with the first buckling mode, must be considered as the limit load of the practical project. It is interesting to note that the vertical straight line in Figure 10 represents the fundamental solution, i.e. the primary instable path.

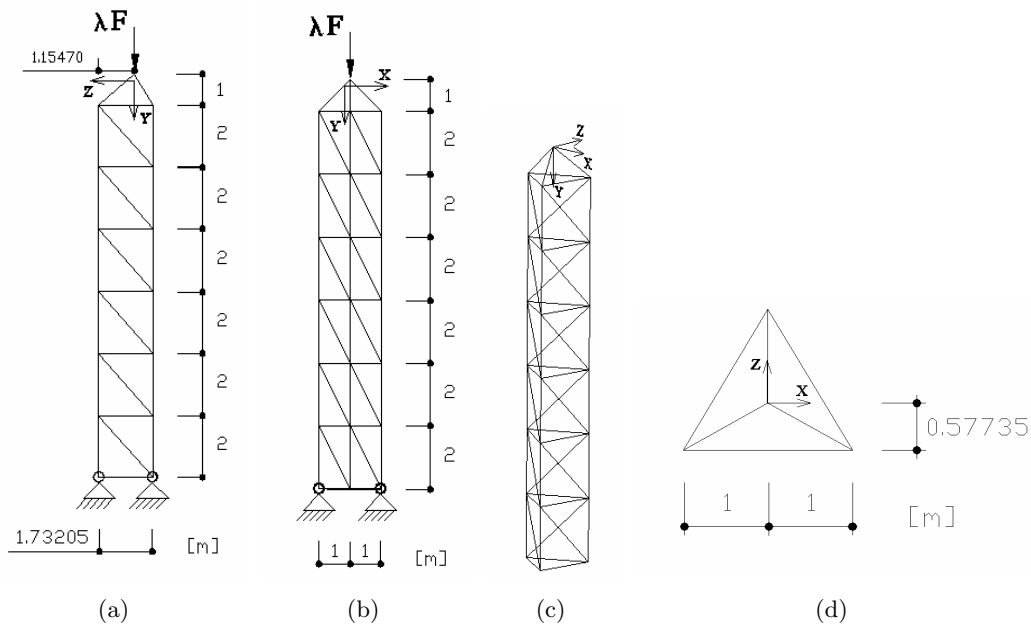


Figure 9: Lateral view (a) front view (b) 3D view (c) top view (d)

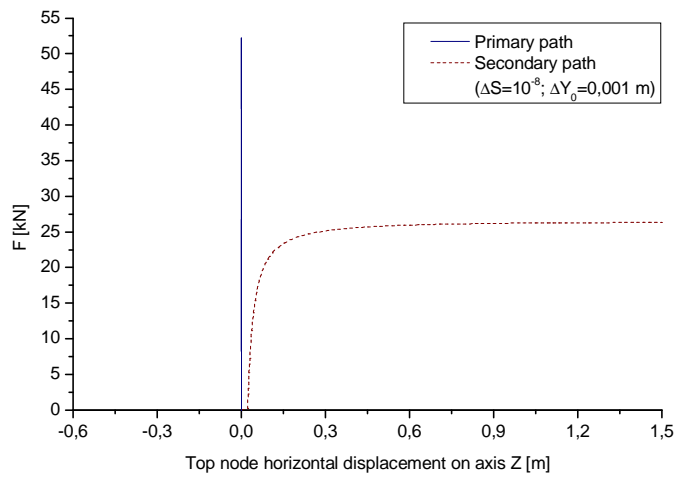


Figure 10: Central node horizontal displacement in direction Z x force

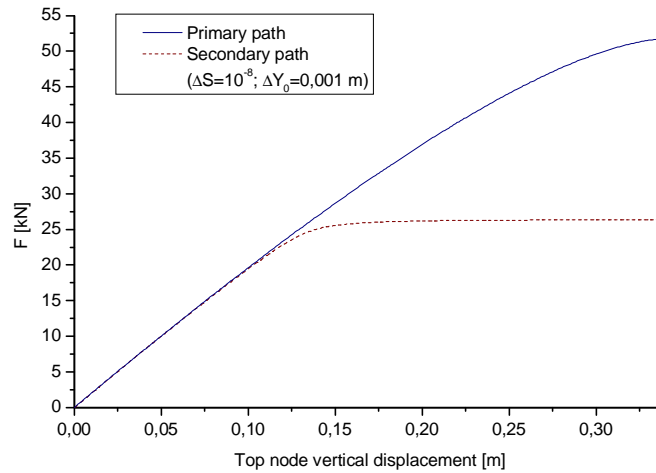


Figure 11: Central node vertical displacement x force

6 Conclusions

The main objective of the paper is to present a simple alternative to the virtual work method to deal with geometrical nonlinear analysis. Due to its simplicity, the method can be easily used by engineers and even structural mechanics students.

The paper presents a formulation based on the Finite Element Method to deal with stability problems in nonlinear analysis. The formulation can be used to analyze severe geometrical nonlinear behavior, including structural post-buckling problems. For practical structural analysis the indirect method used here to obtain the stability points is sufficiently accurate. The accuracy of the formulation has been shown by the four numerical examples presented which have been compared with analytical and other numerical solutions.

The indirect method, the singularity of the Hessian matrix with at least one associated null eigenvalue, is sufficiently acute to find the structural critical stability limits. The negative point of the presented stability analysis is due to the determinant computing during the iterations. The vector iteration method [18] adapted for stability analysis may be recommended to improve the formulation in terms of computer time consuming.

The formulation can be extended easily to the three-dimensional modeling of solids, which simply require carrying out volume integrations over the elements. In this case, three stress components (principal directions) have to be considered to define the energy function and also co-ordinate transforming at the element level is required.

The multiple bifurcations, for which simply the Hessian matrix analysis is not applied, and the dynamic stability, particularly due to its relation with chaos, are still open areas for new contributions.

Acknowledgements: The authors would like to acknowledge FAPESP (São Paulo State Research Foundation) for the financial support.

References

- [1] K.J. Bathe. *Finite element procedures*. Prentice Hall, New Jersey, 1996.
- [2] J.M. Battini, C. Pacoste, and A. Eriksson. Improved minimal augmentation procedure for the direct computation of critical points. *Computer methods in applied mechanics and engineering*, 192:2169–2185, 2003.
- [3] G.E. Blandford. Progressive failure analysis of inelastic space truss structures. *Computers & structures*, 58:981–990, 1996.
- [4] H.B. Coda and M. Greco. A simple fem formulation for large deflection 2d frame analysis based on position description. *Computer methods in applied mechanics and engineering*, 193:3541–3557, 2004.
- [5] M.A. Crisfield. A consistent corotational formulation for nonlinear three-dimensional beam-elements. *Computer methods in applied mechanics and engineering*, 81:131–150, 1990.
- [6] M.A. Crisfield. *Non-Linear finite element analysis of solids and structures*, volume 1. John Wiley & Sons, England, 1991.
- [7] L. Driemeier, S.P.B. Proença, and M. Alves. A contribution to the numerical nonlinear analysis of three-dimensional truss systems considering large strains, damage and plasticity. *Communications in nonlinear science and numerical simulation*, 10:515–535, 2005.
- [8] M.S. Gadala, M.A. Dokainish, and G. A. Oravas. Formulation methods of geometric and material nonlinearity problems. *International journal for numerical methods in engineering*, 20:887–914, 1984.
- [9] M. Greco and H.B. Coda. Positional fem formulation for flexible multi-body dynamic analysis. *Journal of Sound and vibration*, 290:1141–1174, 2006.
- [10] A.E. Green and P.M. Naghdi. A note on invariance under superposed rigid body motions. *Journal of elasticity*, 9:1–8, 1979.
- [11] C.D. Hill, G.E. Blandford, and S.T. Wang. Post-buckling analysis of steel space trusses. *Journal of structural engineering. ASCE*, 115:900–919, 1989.
- [12] M. Kleiber and C. Wozniak. *Nonlinear mechanics of structures*. Kluwer academic publishers, Dordrecht, 1991.
- [13] C.S. Krishnamoorthy, G. Ramesh, and K.U. Dinesh. Post-buckling analysis of structures by three-parameter constrained solution techniques. *Finite elements in analysis and design*, 22:109–142, 1996.
- [14] J.L. Meek and H.S. Tan. Geometrically nonlinear-analysis of space frames by an incremental iterative technique. *Computer methods in applied mechanics and engineering*, 47:261–282, 1984.
- [15] D.P. Mondkar and G.H. Powell. Finite element analysis of non-linear static and dynamic response. *International journal for numerical methods in engineering*, 11:499–520, 1977.
- [16] R.W. Ogden. *Non-linear Elastic deformation*. Ellis Horwood, England, 1984.

- [17] E. Oñate and W.T. Matias. A critical displacement approach for predicting structural instability. *Computer methods in applied mechanics and engineering*, 134:135–161, 1996.
- [18] M. Papadrakakis. Post-buckling analysis of spatial structures by vector iteration methods. *Computers & structures*, 14:393–402, 1981.
- [19] J. Shi. Computing critical points and secondary paths in nonlinear structural stability analysis by the finite element method. *Computers & structures*, 58:203–202, 1996.
- [20] J. Shi and M. Crisfield. A simple indicator and branch switching technique for hidden unstable equilibrium paths. *Finite elements in analysis and design*, 12:303–312, 1992.
- [21] W. Wagner and P. Wriggers. A simple method for the calculation of postcritical branches. *Engineering with computers*, 5:103–109, 1988.
- [22] P. Wriggers and J.C. Simo. A general procedure for the direct computation of turning and bifurcation points. *International journal for numerical methods in engineering*, 30:155–176, 1990.
- [23] P. Wriggers, W. Wagner, and C. Miehe. A quadratically convergent procedure for the calculation of stability points in finite element analysis. *Computer methods in applied mechanics and engineering*, 88:329–347, 1988.
- [24] Y.B. Yang and L.-J. Leu. Postbuckling analysis of trusses with various lagrangian formulations. *AIAA journal*, 28:946–948, 1990.

Appendix

The objectivity of the proposed strain measure should be considered in order to allow the application of the formulation to general large displacements [10, 16].

The general position of points for the analyzed continuum is described by mapping the finite elements, considering an auxiliary dimensionless space with three orthogonal co-ordinates, as shown in Figure A1. The co-ordinate ξ is associated with the element's real axial co-ordinate and P is a general point of the continuum.

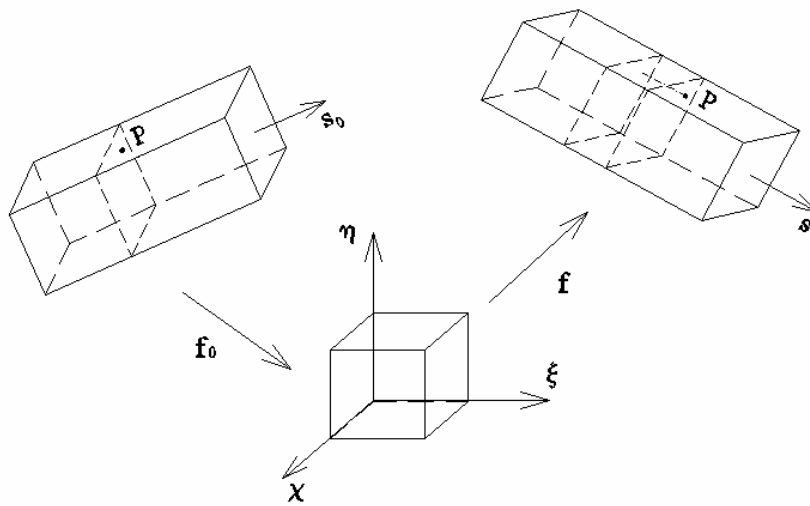


Figure A1: Auxiliary dimensionless space and simple mapping

The mapping represents a deformation from the auxiliary dimensionless space to any real position of the body; therefore the usual non-linear continuum mechanics concepts may be applied. The deformation gradient of this mapping is given by Eq. (A1).

$$A = \begin{bmatrix} \frac{dX_p}{d\xi} & \frac{dX_p}{d\eta} & \frac{dX_p}{d\chi} \\ \frac{dY_p}{d\xi} & \frac{dY_p}{d\eta} & \frac{dY_p}{d\chi} \\ \frac{dZ_p}{d\xi} & \frac{dZ_p}{d\eta} & \frac{dZ_p}{d\chi} \end{bmatrix} \tag{A1}$$

One can compute the stretch λ_ξ for the reference direction ξ defined here by the following unit vector $v_\xi = [1 \ 0 \ 0]^T$ as follows:

$$\lambda_\xi = \lambda(v_\xi) = \left| A \begin{bmatrix} 1 \\ 0 \\ 0 \end{bmatrix} \right| \tag{A2}$$

The other directions are defined by the unit vectors $v_\eta = [0 \ 1 \ 0]^T$ and $v_\chi = [0 \ 0 \ 1]^T$.

It is important to note that for this formulation only the axial direction is considered deformable; therefore it is a principal direction. No strain occurs in the other directions (η and χ).

The proposed strain measure, Eq. (9), is constituted only by the stretch shown in Eq. (A3) and by the constant value $ds_0/d\xi$. Rigid body rotations do not generate strains and therefore the adopted deformation measure is objective, as proved in the references [4,9]

$$\lambda_\xi = \frac{ds}{d\xi} \quad (\text{A3})$$

The limitation of the formulation is that it is suitable only for large displacements analysis, not for large strains analysis. In the second case, a Hyper-elastic constitutive law must be used instead of the Hooke's law or an appropriate strain measure must be used [7,24].